# ARTICLES

## Kramers−Kronig Transformation for Optical Rotatory Dispersion Studies

**Prasad L. Polavarapu**[†]

*Department of Chemistry, Vanderbilt University, Nashville, Tennessee 37235*

*Received: May 10, 2005; In Final Form: June 17, 2005*

The Kramers−Kronig (KK) transform method for deriving optical rotatory dispersion (ORD) from electronic circular dichroism (ECD) has been analyzed. Three different numerical integration methods for the KK transform have been evaluated, and the method proposed by Ohta and Ishida has been used for further calculations. Using this method, the quantum mechanical predictions of electronic circular dichroism (ECD) have been converted to corresponding ORD and compared with that derived from the linear response method. For three molecules exhibiting monosignate ORD in the nonresonant long wavelength region, the KK transform of ECD associated with the lowest energy electronic transition is found to give ORD values close to those obtained with the linear response method. For molecules exhibiting bisignate ORD in the nonresonant long wavelength region, the KK transform method may not provide the correct results. In the resonant region, the KK transform method provides a computationally economical alternative for predicting ORD. While the KK transform method works much like sum-over-states method for ORD, the former offers convenience in transforming the experimental ECD spectrum without the need for spectral curve fitting.

### Introduction

Optical rotation is a well-known technique[1] that is widely practiced in chemical sciences, mostly for the purposes of characterizing the samples. Optical rotatory dispersion (ORD),[2] which is a measure of optical rotation as a function of wavelength, was at one point in time a major area of research in chemical sciences. However, ORD applications did not develop to the level of becoming an attractive tool for structural chemists. The development of instruments for measuring electronic circular dichroism (ECD)[3] in the ultraviolet−visible regions with better sensitivity has for all practical purposes diminished the role of ORD. ECD has been widely used for structural characterization.[3,4] Such characterization in the early days was based mostly on empirical sector rules and spectra−structure correlations, due to the absence of methods for accurate quantitative interpretations of experimental ECD spectra.

It is well-known that ORD and ECD are related via the Kramers−Kronig (KK) transform.[5,6] Thus, if one of these two properties is measured as a function of wavelength then the second can be obtained, at least in principle, via a KK transform. However, such transformation between experimental ECD and ORD has been undertaken[7] rarely, in practice.

The use of optical rotation in structural chemistry was limited due to the lack of an obvious connection between observed rotation and molecular structure. This situation has been changing in the past decade at a rapid pace. Following the first ab initio calculation of optical rotation,[8] numerous advances in quantum theoretical methods for accurately predicting optical rotation, as summarized in recent reviews,[9] have been reported. Different levels of quantum mechanical theories, including Hartree−Fock (HF),[10] density functional theory (DFT),[11] and coupled cluster (CC),[12] have been used for optical rotation predictions. Standard quantum mechanical programs[13] are now available for predicting optical rotation, which led to increased interest in the application of optical rotation for molecular structure determination. If the wavelength at which optical rotation is calculated happens to be at or near the wavelength of an electronic transition, known as resonant region, the quantum mechanical expression for optical rotation becomes singular and optical rotation cannot be calculated in those regions[14] without additional considerations. To avoid singularity, lifetimes of excited states had to be incorporated into the expression. With the inclusion of lifetimes of excited states, it became possible[15] to predict the ORD in the resonant region for chiral molecules of interest. Nevertheless, except for ref 15, the limited number of quantum mechanical ORD studies reported in the literature have either confined to nonresonant region[16] or avoided[14] the resonant region.

Important quantum mechanical advances have also taken place for predicting rotational strengths of electronic transitions, which represent integrated ECD band areas. Here also, HF,[17] DFT,[18] and CC[19] methods have been used for predicting ECD intensities. With the availability of standard quantum mechanical programs[13] for ECD calculations, applications of ECD for reliable predictions of molecular structure are beginning to appear.[20]

The quantum mechanical calculations of ECD and ORD, as undertaken currently, are however independent and use different algorithms. However, as mentioned earlier, ECD and ORD are related via KK transform. Then is it necessary to undertake two separate calculations, one for ECD and another for ORD? Would it not be possible to derive ORD from a given theoretical

[†] Telephone: (615) 322-2836. Fax: (615) 322-4936. E-mail: Prasad.L.Polavarapu@vanderbilt.edu.

10.1021/jp0524328 CCC: $30.25 
Published on Web 07/26/2005

prediction of ECD? If that is possible, then how many ECD bands have to be considered in the KK transform and what restrictions might apply? Meijere et al.[21] did use the KK transform of theoretical ECD to obtain optical rotation at several wavelengths, but the above-mentioned questions were not addressed.

Similar questions apply for experimental data as well. When experimental ORD could not be measured (as for highly absorbing colored samples such as chiral fullerenes) is it not possible to convert the experimental ECD into an ORD spectrum? Since the KK transform can only be achieved with numerical integration methods, which numerical method should be used for converting the experimental ECD into ORD? These questions are addressed in this work, with the objective to find a single KK transform algorithm that can be used to convert both experimental and theoretical ECD into ORD.

The organization of this manuscript is as follows: First the units for ECD and ORD are discussed in order to express them in common units. Although these units have been discussed in the literature, individually for ECD and ORD, multiple sources have to be consulted to see the connection between these units. For pedagogical and reference purposes, these units are summarized first to provide a single reference for future studies. Then three different numerical integration methods available for KK transform between ECD and ORD are summarized. These methods are compared, for the first time, using a single Gaussian ECD band as the test case. One method that is convenient for obtaining the KK transform of both experimental and theoretical ECD has been used for further investigations. Different situations for ORD predictions are discussed and the ORD predictions obtained from KK transform of ECD are compared to those obtained in direct ORD calculations.

## Methods

**Circular Dichroism and Molar Ellipticity.** ECD spectral intensity is expressed[4] as ellipticity in degrees as well as in L mol$^{-1}$ cm$^{-1}$. The theoretical background needed to see the connection between these units is given below. The ellipticity, $\theta$ in radians, is defined[22] as

$$\tan\theta = \frac{E_R - E_L}{E_R + E_L} = \frac{e^{-\alpha_R} - e^{-\alpha_L}}{e^{-\alpha_R} + e^{-\alpha_L}} \quad (1)$$

In eq 1, $E_R$ and $E_L$ are electric field amplitudes for right and left circularly polarized light after passing through the sample; and $\alpha = 2.303\ A/2$, where $A$ is the decadic absorbance. For small values of $\theta$, tan $\theta$ is approximated as $\theta$. Multiplying the numerator and denominator of eq 1 by $e^{(\alpha_R+\alpha_L)/2}$ one obtains,[23]

$$\theta = \frac{e^{(\alpha_L-\alpha_R)/2} - e^{-(\alpha_L-\alpha_R)/2}}{e^{(\alpha_L-\alpha_R)/2} + e^{-(\alpha_L-\alpha_R)/2}} = \tanh(\alpha_L - \alpha_R)/2 \quad (2)$$

For small values of the argument, $\tanh(\alpha_L - \alpha_R)/2 \sim (\alpha_L - \alpha_R)/2$. Thus eq 2 becomes

$$\theta = 2.303\frac{(A_L - A_R)}{4} = \frac{2.303\Delta A}{4} \quad (3)$$

where $\Delta A = A_L - A_R$ is the circular dichroism. Ellipticity can be expressed in degrees by converting eq 3 from radians to degrees,

$$\theta\ (\text{in degrees}) = \frac{2.303\Delta A}{4} \times \frac{180}{\pi} \quad (4)$$

Alternately, circular dichroism $\Delta A$is given as

$$\Delta A = \frac{\theta(\text{in degrees})}{32.988} = \frac{\theta(\text{in millidegrees})}{32988} \quad (5)$$

Using $A = \epsilon cl$, with concentration $c$ in mol/L, path length $l$ in cm, and extinction coefficient $\epsilon$ in L/(mol·cm) one obtains

$$\Delta\epsilon = \frac{\theta(\text{in degrees})}{32.988cl} \quad (6)$$

which is the desired conversion between degrees and L mol$^{-1}$ cm$^{-1}$.

Another commonly used quantity, molar ellipticity $[\theta]$ is defined, in units of deg L/(mol·cm), as

$$[\theta] = \frac{\theta(\text{in degrees})}{cl} = 32.988\Delta\epsilon \quad (7)$$

In units of deg·cm$^2$/dmol, molar ellipticity is given as

$$[\theta] = \frac{\theta(\text{in degrees})}{c\ l} = 3298.8\Delta\epsilon \quad (8)$$

**Rotational Strength and Molar Ellipticity.** The theoretically predicted rotational strengths, which are commonly expressed in units of $10^{-40}$ esu$^2$ cm$^2$, represent the integrated ECD band areas. For the $k$th electronic transition, rotational strength, $R_k$, is given as,[4,24]

$$R_k = \mathrm{Im}\{\langle\psi_0^o|\tilde{\mu}_\alpha|\psi_k^o\rangle\langle\psi_k^o|\tilde{m}_\alpha|\psi_0^o\rangle\} = 22.94 \times 10^{-40}\int\frac{\Delta\epsilon_k(\lambda)\,d\lambda}{\lambda} \approx \frac{22.94\times10^{-40}}{\lambda_k^o}\int\Delta\epsilon_k(\lambda)\,d\lambda \quad (9)$$

where $\psi_0^o$ and $\psi_k^o$ represent the ground and excited electronic state wave functions respectively; $\tilde{\mu}_\alpha$ is the electric dipole moment operator; $\tilde{m}_\alpha$ is the magnetic dipole moment operator and $\Delta\epsilon_k(\lambda)$, in units of L/(mol·cm), is expressed as a function of wavelength $\lambda$. For a Gaussian band with $\Delta\epsilon_k^o$ as the peak intensity, $\lambda_k^o$ as the band center and $\Delta_k$ as half-width at 1/e of peak height, the intensity distribution is given as[25]

$$\Delta\epsilon_k(\lambda) = \Delta\epsilon_k^o e^{-[(\lambda-\lambda_k^o)/\Delta_k]^2} \quad (10)$$

Substitution of eq 10 into eq 9 gives an expression for the peak band intensity$\Delta\epsilon_k^o$ as[25]

$$\Delta\epsilon_k^o = \frac{\lambda_k^o R_k}{22.94\Delta_k\sqrt{\pi}} \times 10^{40} \quad (11)$$

Using the peak intensity $\Delta\epsilon_k^o$ and bandwidth $\Delta_k$, ECD spectral intensity (in units of L/(mol·cm)), at any wavelength can be simulated with a Gaussian intensity profile (eq 10). In practice, though, there will be several electronic transitions, so the intensity distribution from all transitions will have to be summed to obtain the intensity at a given wavelength. Substitution of eqs 9−11 in to eq 8 will convert rotational strength into molar ellipticity.

**Specific Rotation and Molar Rotation.** Specific rotation $[\alpha(\lambda)]$ at wavelength $\lambda$ in units of deg·cm$^3$/(g·dm) is defined as[26]

$$[\alpha(\lambda)] = \frac{100\alpha(\lambda)}{cl} \tag{12}$$

where $\alpha(\lambda)$ is the observed rotation (at wavelength $\lambda$) in degrees, $c$ is the concentration (grams of solute in 100 cm$^3$ of solution), and $l$ is the path length in dm.

In quantum mechanical methods, specific rotation is obtained as[8]

$$[\alpha(\lambda)] = 13.43 \times 10^{-5}\frac{\beta(\lambda)}{\lambda^2 M} \tag{13}$$

where $M$ is molar mass (in g/mol) and the optical rotatory parameter $\beta(\lambda)$ (in atomic units) is obtained as

$$\beta(\lambda) = \frac{1}{3}[\beta_{xx}(\lambda) + \beta_{yy}(\lambda) + \beta_{zz}(\lambda)] \tag{14}$$

where $\beta_{xx}$, related to the electric dipole−magnetic dipole polarizability tensor as[22,27] $\beta_{\alpha\beta} = -\omega^{-1}G'_{\alpha\beta}$, is given, for example, as

$$\beta_{xx}(\lambda) = \frac{1}{h\pi c^2}\sum_{k\#0}\frac{\lambda^2\lambda_k^2}{\lambda^2 - \lambda_k^2}\mathrm{Im}\{\langle\psi_0^o|\tilde{\mu}_x|\psi_k^o\rangle\langle\psi_k^o|\tilde{m}_x|\psi_0^o\rangle\} \tag{15}$$

In eq 15, $\lambda_k = hc/(E_k^o - E_0^o)$ with $E_0^o$ and $E_k^o$ representing the unperturbed energies of ground and excited states, respectively. It is customary to write eqs 13−15 in terms of frequency $\nu$, but here they are written in terms of wavelength to be consistent with other equations. Substituting eqs 9, 14, and 15 into eq 13 gives the sum-over-states (SOS) expression for ORD in the nonresonant region as

$$[\alpha(\lambda)] = \frac{4.477 \times 10^{-5}}{Mh\pi c^2}\sum_k \frac{\lambda_k^2}{\lambda^2 - \lambda_k^2}R_k \tag{16a}$$

Molar rotation $[\varphi(\lambda)]$, in units of (deg·cm$^2$/dmol), is then defined[24,26] as

$$[\varphi(\lambda)] = [\alpha(\lambda)] \times \frac{M}{100} = \frac{4.477 \times 10^{-7}}{h\pi c^2}\sum_k \frac{\lambda_k^2}{\lambda^2 - \lambda_k^2}R_k \tag{16b}$$

The calculation of ORD in the nonresonant region using SOS method has been reported recently.[16e] To calculate ORD in the resonant region, and avoid singularity at $\lambda = \lambda_k$ in eq 16, parts a and b, the denominator in eq 16, parts a and b has to be modified to include the lifetimes of excited states.[15] Following Barron,[22] $1/(\lambda^2 - \lambda_k^2)$can be written as $f + ig$, where $f = (\lambda^2 - \lambda_k^2)/[(\lambda^2 - \lambda_k^2)^2 + \lambda^2\Gamma_k^2]$ and $g = \Gamma_k\lambda/[(\lambda^2 - \lambda_k^2)^2 + \lambda^2\Gamma_k^2]$, where $\Gamma_k$ is the full width of the band at half the maximum height. The real part f contributes[22] only to ORD while the imaginary part contributes[22] to CD. Thus, ORD becomes

$$[\varphi(\lambda)] = \frac{4.477 \times 10^{-7}}{h\pi c^2}\sum_k \frac{\lambda_k^2(\lambda^2 - \lambda_k^2)}{(\lambda^2 - \lambda_k^2)^2 + \lambda^2\Gamma_k^2}R_k \tag{16c}$$

The SOS expressions (eq 16b for nonresonant region only and eq 16c for both resonant and nonresonant regions) indicate that ORD can be obtained from a knowledge of ECD intensities, $R_k$. An alternate approach to convert ECD into ORD is to use the KK transformation as described in the next section.

The sum in eqs 15 and 16a−c extends over infinite number of electronic transitions. This summation over excited states can be avoided using linear response theory.[28] By incorporating excited lifetimes into eq 15 and using linear response theory, one can calculate[15] simultaneously both ORD and ECD at discrete wavelengths respectively as real and imaginary parts. This approach, implemented[15] in the DALTON program, is more accurate than converting ECD into ORD using SOS or KK transform methods.

**Kramers—Kronig Transformation of Molar Ellipticity into Molar Rotation.** Both electronic circular dichroism and optical rotation are expressed, respectively as molar ellipticity and molar rotation, in the same units (deg cm$^2$/dmol), before subjecting them to KK transform. The KK transformation from molar ellipticity $[\theta(\mu)]$ (as a function of wavelength $\mu$) to the molar rotation $[\varphi(\lambda)]$ at wavelength $\lambda$ is given as[24]

$$[\varphi(\lambda)] = \frac{2}{\pi}\int_0^\infty [\theta(\mu)]\frac{\mu}{(\lambda^2 - \mu^2)}\,\mathrm{d}\mu \tag{17}$$

The integration in eq 17 will be truncated to a limited region, because it is not practical to integrate from zero to infinity.

A reviewer has suggested that the KK transform of a truncated ECD spectrum can be shown formally as equivalent to the truncated SOS expression. Then one might wonder about the advantages/disadvantages of using the KK transform. A distinct advantage can be cited for the KK transform as follows. To convert the experimental ECD spectrum into ORD spectrum using eq 16, parts b and c, one has to fit the experimental ECD spectrum to some chosen (Gaussian, Lorentzian, or some other) band profiles and extract the rotational strengths of individual bands. Such tedious spectral curve fitting exercise, and associated inherent ambiguities, can be completely avoided in the KK transform (vide infra), which is a clear advantage. In converting the theoretical ECD band intensities into ORD, however, the KK transform does require ECD spectral simulation using some band profiles (vide infra), while SOS method (eq 16b,c) does not (because theoretical predictions give integrated ECD band areas, as rotational strengths).

The integral on the right-hand side of eq 17 has a singularity at $\lambda = \mu$. To overcome this problem, different numerical methods have been proposed for evaluating this integral. Of these, the most often cited[7] approach is that of Moscowitz[24] and to a lesser extent[7e] is that of Emeis et al.[6] Most convenient method, which has never been used before in the circular dichroism community, however is due to Ohta and Ishida.[29] First we will describe these three methods and compare their performance to establish the method of choice.

**Numerical Integration Methods for KK Transform.** *(A) Moscowitz's Method.*[24] This method assumes a Gaussian intensity profile for ECD bands. For the $k$th ECD band with a Gaussian intensity profile (eq 10), peak intensity $[\theta_k^o]$ and half-width at 1/e of peak height, $\Delta_k$, the ECD intensity at wavelength $\mu$ becomes $[\theta_k(\mu)] = [\theta_k^0]e^{-[(\mu-\mu_k^o)/(\Delta_k)]^2}$. Then the KK transformation for a system with one ECD band (labeled by the subscript $k$) becomes

$$[\varphi_k(\lambda)] = \frac{2[\theta_k^o]}{\pi}\int_0^\infty e^{-[(\mu-\mu_k^o)/(\Delta_k)]^2}\frac{\mu}{(\lambda^2 - \mu^2)}\,\mathrm{d}\mu \tag{18}$$

For bandwidth smaller than the wavelength at band center (i.e $\Delta_k << \mu_k^o$), eq 18 was written[24] to a good approximation as

$$[\varphi_k(\lambda)] = \frac{2[\theta_k^o]}{\pi^{1/2}}\left[e^{-[(\lambda-\lambda_k^o)/(\Delta_k)]^2}\int_0^{\left(\frac{\lambda-\lambda_k^o}{\Delta_k}\right)} e^{x^2}\,dx - \frac{\Delta_k}{2(\lambda+\lambda_k^o)}\right] \quad (19)$$

The integral involved in this equation has been evaluated in the present work using trapezoidal numerical integration by dividing the range from 0 to $(\lambda - \lambda_k^o)/\Delta_k$ into $N$ intervals such that $1/N[(\lambda - \lambda_k^o)/\Delta_k] = h$, as follows:

$$\frac{2[\theta_k^o]}{\pi^{1/2}}[e^{-[(\lambda-\lambda_k^o)/(\Delta_k)]^2}\int_0^{\left(\frac{\lambda-\lambda_k^o}{\Delta_k}\right)} e^{x^2}\,dx] = \frac{2[\theta_k^o]}{\pi^{1/2}}\left[\sum_{x=0}^{\left(\frac{\lambda-\lambda_k^o}{\Delta_k}\right)-h} \frac{[e^{(x+h)^2-[(\lambda-\lambda_k^o)/\Delta_k]^2} + e^{x^2-[(\lambda-\lambda_k^o)/\Delta_k]^2}]}{2}h\right] \quad (20)$$

The value of $x$ in the summation of on the right-hand side of eq 20 changes in increments of $h$ whose magnitude was chosen to be 0.01. For a system with $n$ ECD bands, total molar rotation $[\varphi(\lambda)]$ at wavelength $\lambda$ is obtained by summing over all contributions from $n$ bands. That is

$$[\phi(\lambda)] = \sum_{k=1}^{n}[\phi_k(\lambda)] \quad (21)$$

*(B) Emeis, Oosterhoff, and deVries Method.*[6] The original expressions given by Emeis et al.[6] were in terms of frequencies. Here they are rewritten in terms of wavelength. In this method, eq 17 is rewritten as

$$[\varphi(\lambda)] = \frac{2}{\pi}\int_0^\infty [\theta(\mu)]\frac{\mu}{(\lambda^2-\mu^2)}\,d\mu = \frac{1}{\pi}\left[\int_0^\infty \frac{[\theta(\mu)]}{\lambda-\mu}\,d\mu - \int_0^\infty \frac{[\theta(\mu)]}{\lambda+\mu}\,d\mu\right] \quad (22)$$

On the right-hand side of eq 22, the first integral has a singularity at $\lambda = \mu$. To avoid this singularity, the integral can be broken into three parts as follows:

$$\int_0^\infty \frac{[\theta(\mu)]}{\lambda-\mu}\,d\mu = \int_0^{\lambda-\delta} \frac{[\theta(\mu)]}{\lambda-\mu}\,d\mu + \int_{\lambda-\delta}^{\lambda+\delta} \frac{[\theta(\mu)]}{\lambda-\mu}\,d\mu + \int_{\lambda+\delta}^\infty \frac{[\theta(\mu)]}{\lambda-\mu}\,d\mu \quad (23)$$

In practice, the integration limits of 0 and infinity cannot be realized, so we have to restrict the integration to a finite region, e.g., from $a$ to $b$. Substituting eq 23 into eq 22, one obtains

$$[\varphi(\lambda)] = \frac{1}{\pi}\left[\int_a^{\lambda-\delta} \frac{[\theta(\mu)]}{\lambda-\mu}\,d\mu + \int_{\lambda-\delta}^{\lambda+\delta} \frac{[\theta(\mu)]}{\lambda-\mu}\,d\mu + \int_{\lambda+\delta}^b \frac{[\theta(\mu)]}{\lambda-\mu}\,d\mu - \int_a^b \frac{[\theta(\mu)]}{\lambda+\mu}\,d\mu\right] \quad (24)$$

Emeis et al. suggested[6] that these integrals can be evaluated using a numerical procedure by dividing the range from $a$ to $b$ into $N$ equal intervals, $h = (b - a)/N$, and using $[\theta(\mu)]$ values at odd multiples of $h/2$ intervals as follows:

$$\frac{1}{\pi}\int_a^{\lambda-\delta} \frac{[\theta(\mu)]}{\lambda-\mu}\,d\mu + \int_{\lambda+\delta}^b \frac{[\theta(\mu)]}{\lambda-\mu}\,d\mu \approx \frac{1}{\pi}\sum_{k=1}^{N}{}^{\#}\frac{[\theta(a+kh-h/2)]}{n-k} \quad (25)$$

$$-\frac{1}{\pi}\int_a^b \frac{[\theta(\mu)]}{\lambda+\mu}\,d\mu \approx -\frac{1}{\pi}\sum_{k=1}^{N}\frac{[\theta(a+kh-h/2)]}{n+k} \quad (26)$$

$$\frac{1}{\pi}\int_{\lambda-\delta}^{\lambda+\delta} \frac{[\theta(\mu)]}{\lambda-\mu}\,d\mu = \frac{1}{\pi}\left[-2\delta\theta'(\lambda) - \frac{1}{9}\delta^3\theta'''(\lambda)\right] \quad (27)$$

where $\theta'(\lambda) = \{d[\theta(\lambda)]\}/d\lambda$ and $\theta'''(\lambda) = \{d^3[\theta(\lambda)]\}/d\lambda^3$; the # sign on the summation in eq 25 indicates that the term with $n=k$ is omitted. Then the molar rotation at a wavelength, $\lambda = a + nh - h/2$, is obtained by substituting eqs 25−27 into eq 24.

In the practical implementation of this method, eq 24 was calculated for each ECD band, whose $[\theta(\mu)]$ was simulated with Gaussian intensity distribution and total molar rotation was obtained as in eq 21 by summing over contributions from all ECD bands. The derivatives in eq 27 have been obtained in the present work using a 4-point numerical derivative formulas given by Emeis et al.[6]

*(C) Ohta and Ishida's Method.*[29] The KK transform between absorption and refractive index as discussed by Ohta and Ishida has been adopted here for molar ellipticity and molar rotation. The original equations[29] of Ohta and Ishida, written in terms of wavenumbers, are rewritten here in terms of wavelength. Assuming that the ECD spectrum is available at constant intervals of h and that the wavelengths and spectral intensities at these intervals are labeled, respectively, as $\mu_j$ and $[\theta(\mu_j)]$ with $j = 1, 2, ..., N$, eq 17 can be approximated, following Ohta and Ishida, as

$$[\varphi(\lambda)] = \frac{2}{\pi}\int_0^\infty [\theta(\mu)]\frac{\mu}{(\lambda^2-\mu^2)}\,d\mu \approx \left(\frac{2}{\pi}\right)(2h)\left(\frac{1}{2}\right)\sum_j{}^{\#}\left[\frac{[\theta(\mu_j)]}{\lambda-\mu_j} - \frac{[\theta(\mu_j)]}{\lambda+\mu_j}\right] \quad (28)$$

In this equation, the summation $\Sigma^{\#}$ signifies that the summation uses alternate data points to avoid singularity at $\lambda = \mu$. If the wavelength $\lambda$, where molar rotation is to be calculated, corresponds to an odd data number, then the summation is carried over even data numbers. On the other hand if the wavelength where molar rotation is to be calculated corresponds to an even data number, then the summation is carried over odd data numbers. Equation 28, referred to by Ohta and Ishida as Maclaurin's formula, is the easiest to implement among the three methods discussed. Ohta and Ishida also showed[29] that among several numerical methods that they evaluated, eq 28 provided least deviation from the exact KK transform.

It should be noted that eq 28 has never been applied before for converting ECD to ORD. In the practical implementation, eq 28 was calculated for each ECD band, whose $[\theta(\mu)]$ was simulated with Gaussian intensity distribution and total molar rotation was obtained as in eq 21 by summing over contributions from all ECD bands.

## Results

**Comparison of the Numerical Integration Methods.** We are not aware of any previous comparison in the literature of

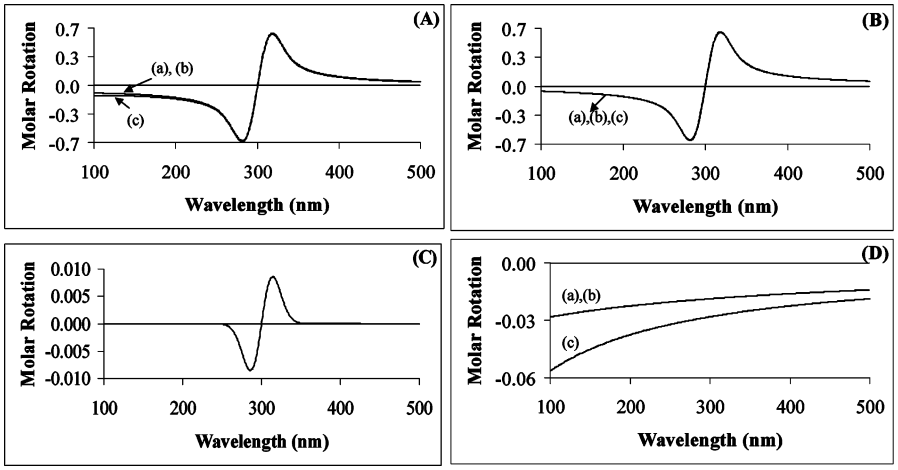


**Figure 1.** (A) Comparison of different numerical integration methods for the KK transformation of one Gaussian circular dichroism band. Traces a and b were obtained using eqs 28 and 19, respectively; trace c was obtained using eq 24. (B) Comparison of major contribution terms in different numerical integration methods: eq 20 for Moscowitz's method, eq 25 for the method of Emeis et al., and the first term in eq 28 for Ohta and Ishida's method. All three curves fall on top of each other, so they cannot be distinguished. (C) Contribution from the third term (eq 27) in the method of Emeis et al. (D) Contribution from the second terms in different methods. Traces a and b were obtained from the second terms in eqs 19 and 28, respectively. Trace c was obtained from eq 26. For all of the traces, one ECD band with $\lambda_k^o = 300$ nm; $[\theta_k^o] = 1$ deg·cm$^2$/dmol; $\Delta_k = 20$ nm, and Gaussian intensity distribution were used.

the three methods discussed above. Moscowitz's method is specific for Gaussian intensity distribution, while the remaining two methods are applicable for any ECD spectral data available at constant intervals. To provide a common data set for all three methods, Gaussian intensity distribution is assumed for the ECD bands that were used to obtain the numerical KK transform. For a quantitative comparison of these methods, root-mean-square percent difference (RMSP) will be used which is defined as

$$\mathrm{RMSP} = \sqrt{\frac{1}{N}\sum_{i=1}^{N}\left[\frac{\{[\phi(\lambda_i)]_1 - [\phi(\lambda_i)]_2\}}{0.5\{[\phi(\lambda_i)]_1 + [\phi(\lambda_i)]_2\}}x100\right]^2} \quad (29)$$

where $[\phi(\lambda_i)]_1$ and $[\phi(\lambda_i)]_2$are the molar rotations obtained in two different methods, 1 and 2 respectively, at wavelength $\lambda_i$. However, eq 29 can only be used to compare the methods of Moscowitz and Ohta and Ishida, because wavelength increment for the ORD calculations with these two methods is an integer multiple of interval h. In the method of Emeis et al., this wavelength increment is an odd multiple of $h/2$.

To compare the three numerical methods, the KK transform of a single Gaussian ECD band was considered as a test case with the following parameters. $\lambda_k^o = 300$ nm; $[\theta_k^o] = 1$ deg cm$^2$/dmol and $\Delta_k = 20$ nm; integration range = 100−500 nm. The results are shown in Figure 1A, where traces a−c were obtained using the methods of Moscowitz,[24] Ohta and Ishida,[29] and Emeis et al.,[6] respectively. It is apparent that two methods, that due to Moscowitz and that due to Ohta and Ishida, give essentially the same result, but the third method, due to Emeis et al., gives somewhat different results, especially at shorter wavelengths. The root-mean-square percent difference between Moscowitz and Ohta and Ishida's mehods is 0.14.

To obtain further insight into the source for the differences among these methods, individual contributions from different terms in each of the three methods were analyzed. For this purpose the same parameters as those used to obtain Figure 1A were used. Molar rotation has contributions from two terms in Moscowitz's method (the first and second terms in eq 19), three different terms (eqs 25−27) in the method of Emeis et al. and two terms (the first and second terms in eq 28) in the method of Ohta and Ishida. It is found that the major contributions to molar rotation in all three methods (eq 20, eq 25, and the first term in eq 28) are all identical (see Figure 1B). The contribution from the third term (eq 27) in the method of Emeis et al. (see Figure 1C) has a shape similar to that of the first term (eq 25) but is of very small magnitude (maximum values of $\pm 8 \times 10^{-3}$ around the band center for the band parameters used in Figure 1). Then the difference (Figure 1A) noted in the short wavelength region between the method of Emeis et al. and other two methods must originate from eq 26 and the second terms in eqs 19 and 28. Contribution from the second term in eq 19 (Moscowitz's method) is *negative* with its magnitude increasing at shorter wavelengths (Figure 1D, $-2.8 \times 10^{-2}$ at 200 nm) and is identical to that from the second term in eq 28 (Ohta and Ishida's method). The root-mean-square percent difference between Moscowitz and Ohta and Ishida's mehods for this second term is $7 \times 10^{-2}$. Although eq 26 (method of Emeis et al.) gives the same trend as the second terms in eqs 19 and 28, the magnitude of the contribution from eq 26 is larger ($-5.6 \times 10^{-2}$ at 200 nm for band parameters in Figure 1A). Thus, the main difference between the method of Emeis et al. and the other two methods comes from a larger magnitude contribution from eq 26 at shorter wavelengths. From the above discussion it can be seen that the results of Moscowitz's method (eq 19) are identical to those obtained with the method of Ohta and Ishida (eq 28).

For converting theoretical ECD spectrum into ORD, one can use KK transform (eq 19 or eq 28) or SOS expression (eq 16b,c). The use of eq 19 requires the use of Gaussian band profiles for ECD bands, but eq 28 can be used with any band profile. For transforming the experimental ECD spectrum (where data are digitized at constant intervals) into ORD, it is advantageous to use eq 28 over SOS expression (eq 16b,c) because raw experimental data can be used as such with eq 28. However, to use the SOS expression (eq 16b,c), one has to fit the experimental ECD spectrum to some chosen band profiles and extract the integrated areas (rotational strengths) of individual ECD bands, which will be influenced by the inherent ambiguities associated with the curve fitting procedures.

**TABLE 1: Comparison of Molar Rotations (deg·cm²/dmol) Obtained with Linear Response and KK Transform[a] Methods for (*R*)-3-Chloro-1-butyne**

| | B3LYP/6-31G* | | B3LYP/aug-cc-pVDZ | | B3LYP/6-31++G(2d,2p) | | B3LYP/aug-cc-pVTZ | |
|---|---|---|---|---|---|---|---|---|
| wavelength (nm) | linear response | KK transform | linear response | KK transform | linear response | KK transform | linear response | KK transform |
| 633 | 13.5 | 11.6 | 22.9 | 26.8 | 13.5 | 23.4 | 20.6 | 24.4 |
| 589 | 16.5 | 13.7 | 27.5 | 31.6 | 16.5 | 27.6 | 24.7 | 28.8 |
| 546 | 20.6 | 16.3 | 33.4 | 37.9 | 20.6 | 33 | 30.1 | 34.4 |
| 436 | 42.9 | 28.7 | 63.4 | 67 | 42.9 | 58.1 | 57.4 | 60.5 |
| 405 | 56.4 | 35.2 | 80.4 | 82.2 | 56.4 | 71.2 | 72.9 | 74 |
| 365 | 86.1 | 45.1 | 116.3 | 113 | 86.1 | 97.5 | 105.7 | 101.2 |

[a] Using ECD of lowest energy electronic transition.

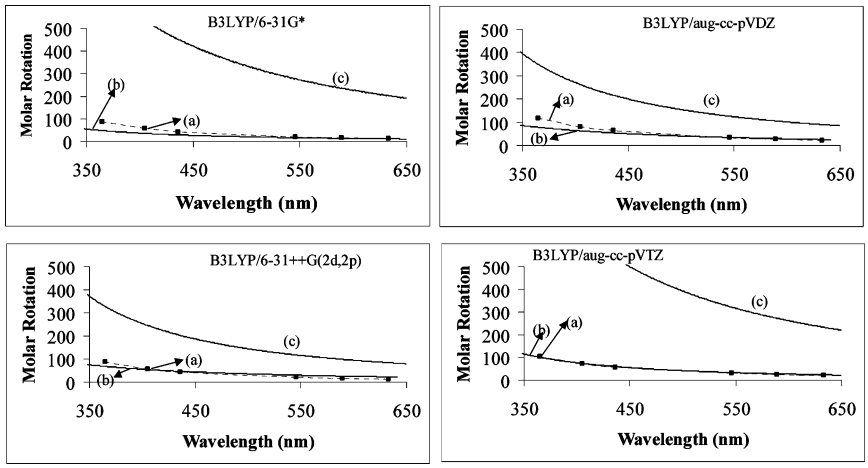


**Figure 2.** Comparison of ORD for (*R*)-3-chloro-1-butyne obtained from linear response method (a) with those obtained from KK transform of ECD (b, c) The calculations were performed at B3LYP/6-31G* (top left panel), B3LYP/aug-cc-pVDZ (top right panel), B3LYP/6-31++G(2d,2p) (bottom left panel), and B3LYP/aug-cc-pVTZ (bottom right panel) level. Theoretical ECD spectra were simulated with Gaussian intensity profile with 20 nm half-width at 1/e of peak height. Trace b was obtained from the ECD of the lowest energy electronic transition. Trace c was obtained from the ECD of the first 25 electronic transitions.

From the information provided above, it can be seen that eq 28 represents a single algorithm that can be used for all of the following needs: (a) Digitized experimental ECD can be converted to ORD without the need for spectral curve fitting. (b) Theoretical ECD can be converted to ORD, in both resonant and nonresonant regions, using a chosen intensity distribution (Gaussian, Lorentzian, etc.) for theoretical ECD spectra.

**Comparison of ORD Derived from KK Transform and Linear Response Methods.** In the following sections, ORD derived from eq 28 will be compared to that obtained from the linear response method. For optical rotation calculations using linear response method, this method as implemented in the Gaussian 03 program[13a] was used. The same program was used for calculating the rotational strengths of electronic transitions. In each case, the molecular geometry was optimized at the same theoretical level as that used for predicting rotational strengths and optical rotation. To apply the KK transform method using eq 28, the theoretical ECD spectra were simulated with Gaussian band profiles with $\Delta_k = 20$ nm. Since the predicted electronic transitions for any of the molecules considered did not occur at shorter wavelength than 100 nm, a integration range of 100−650 nm was used in the KK transform. In some cases where electronic transitions included in the KK transform occurred close to 100 nm, integration range was extended to 10−650 nm, but that did not significantly change the results shown here.

The ORD results obtained from the KK transform depend on the number of electronic transitions used. In principle one should use, although physically impossible, an infinite number of electronic transitions in the KK transform. However, practical reasons dictate that only a finite number of electronic transitions can be used. Even in this finite number, there is no a priori criterion to choose a certain number of electronic transitions. For this reason, we make two choices: (a) use only the first lowest energy electronic transition; (b) arbitrarily use the first 25 electronic transitions. There is no specific reason for choosing 25 transitions, and one could have equally chosen 10 or 50 transitions. ORD obtained with these two choices will be compared to that obtained with the linear response method, considering three different situations: (a) monosignate ORD in the long wavelength region where no electronic transitions appear; (b) bisignate ORD also in the long wavelength region where no electronic transitions appear; (c) ORD in the resonant wavelength region.

*(A) Monosignate ORD in the Nonresonant Long Wavelength Region. (R)-3-chloro-1-butyne.* For this molecule, calculations were carried out using B3LYP functional and four different basis sets, namely 6-31G*, aug-cc-pVDZ, 6-311++G(2d,2p), and aug-cc-pVTZ, and the results are shown in Table 1 and Figure 2. In this figure, trace a was obtained with linear response method, trace b with the KK transform of ECD associated with the lowest energy transition, and trace c with KK transform of ECD associated with the first 25 electronic transitions. It is apparent that the KK transform of ECD associated with lowest energy transition yields ORD that matches nearly quantitatively (see aug-cc-pVTZ results in Table 1) with that obtained from linear response method; ORD magnitudes obtained from the KK transform of ECD associated with the first 25 electronic transitions deviate significantly (see Figure 2). The following statement can rationalize these observations. Since ORD for (*R*)-3-chloro-1-butyne in the 350−650 nm region determined from

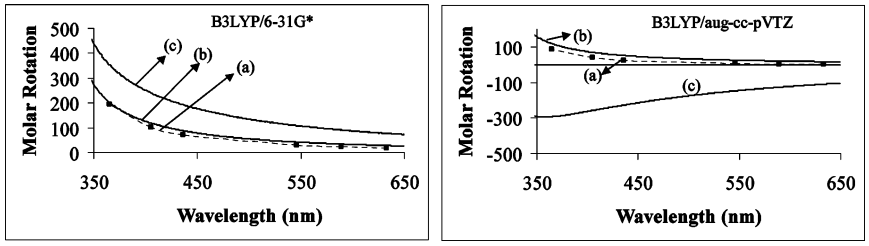


**Figure 3.** Comparison of ORD for (*R*)-3-methylcyclohexanone obtained from linear response method (a) with that obtained from KK transform of ECD (b, c). The calculations were performed at B3LYP/6-31G* (left panel) and B3LYP/aug-cc-pVTZ (right panel). Theoretical ECD spectra were simulated with Gaussian intensity profile with 20 nm half-width at 1/e of peak height. Trace b was obtained from the ECD of lowest energy electronic transition. Trace c was obtained from the ECD of the first 25 electronic transitions.

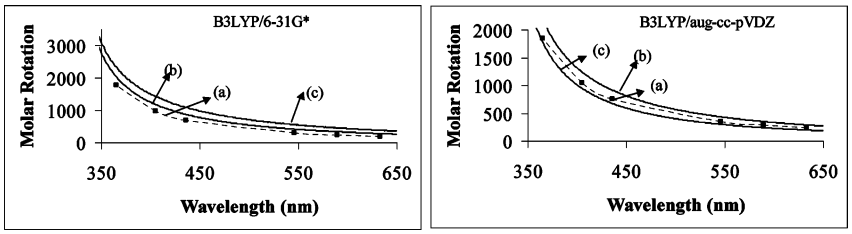


**Figure 4.** Comparison of ORD for (*R*)-3-methylcyclopentanone obtained from linear response method (a) with that obtained from KK transform of ECD (b, c). The calculations were performed at B3LYP/6-31G* (left panel), B3LYP/aug-cc-pVDZ (right panel). Theoretical ECD spectra were simulated with Gaussian intensity profile with 20 nm half-width at 1/e of peak height. Trace b was obtained from the ECD of lowest energy electronic transition. Trace c was obtained from the ECD of the first 25 electronic transitions.

the KK transform of ECD associated with the first electronic transition reproduced satisfactorily that obtained from linear response method, the net sum of ORD contributions to this region from all of the remaining high energy electronic transitions must have been small (or nearly zero). When ECD associated with a finite number of electronic transitions, beyond the lowest energy transition, is used in the KK transform erroneous ORD can result due to inadequate compensation among the finite number of transitions considered.

*(+)-(R)-3-Methylcyclohexanone*: Calculations were carried out for equatorial-methyl conformer in the chair form using B3LYP functional and three different basis sets, namely 6-31G*, aug-cc-pVDZ, and aug-cc-pVTZ. The results obtained with 6-31G* and aug-cc-pVTZ basis sets are shown in Figure 3. The results obtained with aug-cc-pVDZ basis set are similar to those obtained with aug-cc-pVTZ basis set and are not shown. As before, trace a was obtained with the linear response method, trace b with the KK transform of ECD associated with the lowest energy transition, and trace c with the KK transform of ECD associated with the first 25 electronic transitions. In both calculations, the KK transform of ECD associated with the lowest energy transition yields ORD magnitudes that are similar to those obtained with linear response method. However, ORD magnitudes obtained from the KK transform of ECD associated with the first 25 electronic transitions differ significantly. In the case of aug-cc-pVTZ calculation, a negative ORD with increasing magnitude at shorter wavelength is obtained, which is just opposite to that obtained with 6-31G* basis set and also with the linear response method. These observations suggest that, since ORD for (+)-(*R*)-3-methylcyclohexanone in the 350−650 nm region determined from the KK transform of ECD associated with the first electronic transition reproduced satisfactorily that obtained from linear response method, the net sum of ORD contributions to this region from all of the remaining high energy electronic transitions must have been small. When ECD associated with a finite number of electronic transitions, beyond the lowest energy transition, is used in the KK transform, erroneous ORD can result due to inadequate compensation among the finite number of transitions considered.

*(+)-(R)-3-Methylcyclopenatnone.* Calculations were carried out for equatorial-methyl conformer using B3LYP functional and two different basis sets, namely 6-31G* and aug-cc-pVDZ, and the results are shown in Figure 4. As before, trace a was obtained with the linear response method, trace b with the KK transform of ECD associated with the lowest energy transition, and trace c with the KK transform of ECD associated with the first 25 electronic transitions. In the B3LYP/6-31G* calculation, the KK transform of ECD associated with either lowest energy transition or the first 25 transitions yields ORD whose magnitudes are only slightly larger than those obtained with linear response method. In the B3LYP/aug-cc-pVDZ calculation also, the KK transform of ECD associated with either the lowest energy transition or the first 25 transitions yields ORD magnitudes that are only slightly different from those obtained with the linear response method. These observations can be rationalized by the following statement. Since ORD for (+)-(*R*)-3-methylcyclopenatnone in the 350−650 nm determined from the KK transform of ECD associated with the first electronic transition reproduced satisfactorily that obtained from linear response method, the net sum of ORD contributions to this region from all of the remaining higher energy electronic transitions must have been small.

For the three molecules considered above, it is evident that, for monosignate ORD in the nonresonant long wavelength region, the KK transform of ECD associated with the first lowest energy electronic transition reproduces the ORD obtained with linear response method quite well. However, this should not be construed as a generally applicable result (vide infra).

*(B) Bisignate ORD in the Nonresonant Long Wavelength Region.* The origin of bisignate ORD in the resonant region is well understood because, as can be seen in Figure 1A, ORD changes sign at the wavelength of electronic transition. One should be aware that bisignate ORD can also occur in the nonresonant long wavelength region, due to opposing ORD contributions from ECD associated with different electronic transitions situated at shorter wavelengths. To illustrate this point, a simulated ORD resulting from a positive ECD band centered at 300 nm and a negative ECD band centered at 200

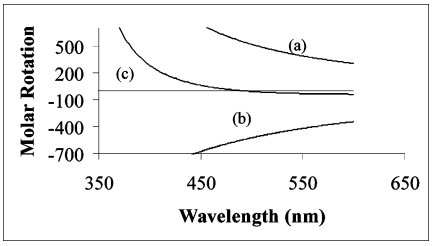


**Figure 5.** Simulation of bisignate ORD in the nonresonant long wavelength region. (a) ORD from positive Gaussian ECD band centered at 300 nm. (b) ORD from negative Gaussian ECD band centered at 200 nm with a 3 times larger magnitude of rotational strength. (c) Total ORD resulting from the overlapping contributions of parts a and b. The ORD sign change occurs at 488 nm, Both ECD bands were assumed to have half-width of 20 nm at 1/e of peak height.

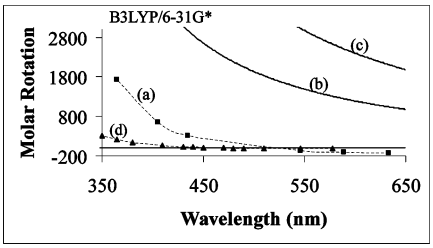


**Figure 6.** Comparison of ORD for (*S*)-(−)-3,3,3′,3′-tetramethyl-1,1′-spirobi[3H,2,1]-benzoxaselenole obtained from the linear response method (a) with those obtained from the KK transform of ECD (b, c). Trace d shows the experimental data from ref 31. The calculations were performed at B3LYP/6-31G*. Theoretical ECD spectra were simulated with Gaussian intensity profile with 20 nm half-width at 1/e of peak height. Trace b was obtained from the KK transform of ECD associated with the lowest energy electronic transition. Trace c was obtained from the KK transform of ECD associated with the first 25 electronic transitions.

nm (with magnitudes of rotational strength in 1:3 ratio) is shown in Figure 5. Both ECD bands were assumed to have half-widths of 20 nm at 1/e of peak height. The total ORD is seen to change sign at 488 nm, where there is no electronic transition. Such reversal of ORD sign, at a wavelength far from the electronic transitions, is actually observed[14b,30−32] in the experimental data for some molecules. Such cases are problematic for theoretical predictions, because (except for fortuitous cases) very accurate calculations are often needed to correctly reproduce the ORD sign reversal in the nonresonant long wavelength region. Some examples include $\beta$-pinene[14b,30] and 3,3,3′,3′-tetramethyl-1,1′-spirobi[3H,2,1]-benzoxaselenole[31] (spiroselenurane, for short) and methyloxirane.[32] For spiroselenurane, electronic transitions appear at wavelengths shorter than 285 nm. However, experimental ORD[31] changes sign at 475 nm (Figure 6, trace d). Linear response method calculation at B3LYP/6-31G* level (Figure 6, trace a) does predict[31] sign reversal in ORD for this molecule [which is probably fortuitous because higher level calculation at B3LYP/6-31+G does not predict[31] this sign reversal]. The KK transform of ECD obtained at the same B3LYP/6-31G* level, however, predicts only monosignate ORD regardless of using the ECD associated with the first lowest energy transition (Figure 6, trace b) or the first 25 low energy electronic transitions (Figure 6, trace c). It is not clear how to choose the number of electronic transitions needed to reproduce the sign reversal in ORD and as a result KK transform approach fails here. However, the linear response method also fails for spiroselenurane at B3LYP/6-31+G level. The difficulties with the linear response method for $\beta$-pinene[14b,30] and methyloxirane[32] in reproducing the bisignate ORD in the nonresonant long wavelength region have been documented in the literature. Thus, a correct prediction of bisignate ORD in the nonresonant long wavelength region is a challenge for both KK transform and linear response methods.

*(C) ORD in the Resonant Wavelength Region.* In the wavelength region where electronic transitions occur, ORD contributions from the ECD associated with transitions situated at far away wavelengths will be secondary (unless their ECD intensities turn out to be unusually large) compared to those from ECD associated with transitions in the resonant region. Therefore, for the KK transformation, it is sufficient to consider just those electronic transitions that appear in (and perhaps, in the immediate vicinity of) the resonant region under investigation. For ORD predictions in the resonant region, the KK transform method might be advantageous over the linear response method for reasons of computational time (vide infra).

One example[33] for this category that is currently under investigation is $C_{76}$. Here, ORD in the resonant region obtained from the KK transform of DFT predicted ECD is found[33] to be in agreement with that predicted using linear response method at the same theoretical level as well as with the ORD derived from the KK transform of experimental ECD.

## Discussion

For predicting ORD in the nonresonant long wavelength region, where no electronic transitions appear, the three simple molecules ((*R*)-3-chloro-1-butyne, (*R*)-3-mehylcyclohexanone, and (*R*)-3-methylcyclopenatnone) considered indicate that the KK transform of ECD associated with the lowest energy transition gives essentially the same result as that obtained from the linear response method. It should be stressed here that *one should not expect to see this behavior in general* and should not expect to obtain quantitatively accurate numbers from the KK transform of ECD associated with one electronic transition. The same statements apply for deriving ORD using SOS method (eq 16b,c). Nevertheless, it is interesting to note that the magnitudes of ORD obtained this way are quite close to those obtained in the linear response method. Since the latter method indirectly accounts for an infinite number of electronic transitions, it appears that the sum of ORD contributions from the electronic transitions beyond the first is either nearly zero or small. This is an important observation because if the same behavior upholds in other molecules that also exhibit monosignate ORD in the nonresonant long wavelength region, then prediction of ORD is obtained trivially from ECD of one transition. If the sign of monosignate ORD in the nonresonant long wavelength region is opposite to that of ECD associated with lowest energy transition, then multiple transitions have to be included in both KK transform and SOS methods. However, then it is not clear how to truncate the number of electronic transitions to be considered with these methods.

When a finite number of electronic transitions are included in the KK transform, for the molecules considered here, the predicted ORD is found to deviate significantly from that obtained with linear response method. One would see the same behavior with SOS method (eqs 16b,c), because the final result in SOS method also depends on where the summation is truncated. The reason for this is an inadequate compensation among the transitions included in both KK transform and SOS methods. As the number of electronic transitions considered is increased, one would essentially be probing the transitions into continuum, so the high-energy transitions occur very close to each other. As a result the compensation among ORD contributions from these high-energy transitions becomes ill-defined.

For molecules, which fall into the category of monosignate ORD in the nonresonant wavelength region, and also possess

the same sign for ECD of lowest energy transition, the emphasis should be on predicting the ECD of lowest energy transition accurately. In these cases, both KK transform and SOS methods do not yield any new information. However, to ascertain that a given molecule belongs to this category, both experimental ORD and ECD spectra should have been measured in the first place.

If bisignate ORD is either experimentally observed or theoretically predicted, in the nonresonant long wavelength region where there are no electronic transitions, then that is a clear indication of oppositely signed ORD contributions from two or more electronic transitions situated at shorter wavelengths. Such ORD pattern is difficult to predict with KK transform and SOS methods because of the uncertainty in the number of electronic transitions that one has to consider. A similar difficulty exists with the linear response method as well, because a delicate balance between opposing ORD contributions has to be correctly reproduced in the calculations, which amounts to predicting correct relative positions of electronic transitions and associated rotational strengths. For such cases,[14b,30−32] it may become necessary to use higher theoretical levels that can correctly represent the excited electronic states.

In the resonant wavelength region, ORD predictions using the KK transform method are probably advantageous over the linear response method. For applying the KK transform method it is sufficient to consider only those electronic transitions that appear in the resonant region being considered. To correctly reproduce the ORD in the edges of that region, it might be necessary to also include the transitions in the immediate vicinity of that region. The linear response method, however, amounts to including infinite number of electronic transitions, requiring much more computational time. With the Gaussian 03 program on a IBM P690 cluster of computers with eight processors at the University of Illinois, optical rotation calculation at a single wavelength for $C_{76}$ using the B3LYP/6-31G* theory required 477 h of clock time. To calculate ORD at several wavelengths, the corresponding time would be much higher. On the other hand, the ECD calculation for the first 25 electronic transitions required only 70 h of clock time. At the HF/6-31G* level, the corresponding times for $C_{76}$ were 80 and 57 h, respectively. Even when OR calculation at a single wavelength required the same amount of time as ECD calculation for several transitions, ORD calculations using the linear response method would be time demanding because OR calculations are required at several wavelengths. Thus, for such large systems, KK transform method can make ORD calculations possible in situations where the calculation of ORD with the linear response method may not be feasible (at least for those who do not have access to supercomputing facilities). It should be pointed out that the advantages mentioned in this paragraph for KK transform method will also apply to SOS method (eqs 16b,c).

It is important to note that the magnitudes of ORD obtained in the KK transform and SOS methods are only approximate because of the limited number of electronic transitions used. For quantitatively accurate estimates of ORD magnitudes, the linear response method is to be preferred. In all three cases of ORD mentioned above, the measurement of ORD is a prerequisite to identify the category to which a given molecule belongs.

There has been considerable discussion[34] in the literature regarding the errors associated with predicted optical rotation magnitudes. Most of these discussions are based on predicting optical rotation magnitudes at a single wavelength, 589 nm. For the noted differences between predicted and experimental magnitudes, various sources such as basis set errors,[35] solvent influence,[36] solute−solute interactions,[37] and/or vibrational corrections[38] are being considered. However an important source that has not been addressed thus far in the literature is the *wavelength correction*. Calculated electronic transitions may appear[39] at shorter (for Hartree−Fock methods) or longer (for B3LYP density functional methods) wavelengths, relative to the experimentally observed transition wavelengths. As an example, the experimental ECD spectrum[40] of (+)-(*R*)-3-chloro-1-butyne is compared to those predicted using B3LYP functional and different basis sets in Figure 7. As can be seen in this figure, B3LYP predicted positive ECD band appears at longer wavelength, (namely 204, 215, and 213 nm respectively in 6-31G*, aug-cc-pVDZ, and aug-cc-pVTZ calculations) compared to the corresponding experimental band at 192 nm. In such cases the experimentally measured optical rotation value at 589 nm does not correspond to the calculated optical rotation value at 589 nm. Instead, calculation of optical rotation should be done at a wavelength *shifted* from 589 nm, to account for the difference between calculated and experimentally observed electronic transition wavelengths. Such wavelength corrections are mandatory for quantitative comparisons but have not been addressed to date in the literature. A problem in making wavelength corrections is that the wavelength shift may vary for different transitions and experimental data may be limited to a certain region (as was the case for 3-chloro-1-butyne). In that case one would have to estimate an *effective wavelength* shift. This problem is circumvented in the ORD studies, where one can see the trend in optical rotations as a function of wavelength and shift the whole curve as needed in relation to the experimental data. In fact in this manner one may be able to determine the *effective wavelength correction*. As an example, comparison of the experimental ORD (trace d, Figure 6) with the B3LYP/6-31G* predicted ORD using linear response method (trace a, Figure 6) for selenurane[31] indicates that the sign reversal in the experimental ORD curve occurs at 475 nm, while that in the predicted ORD curve occurs at ∼524 nm, indicating an *effective wavelength correction* of ∼49 nm. This would mean that the experimental optical rotation at 589 nm for this molecule is better compared to that calculated at 638 nm, not at 589 nm.

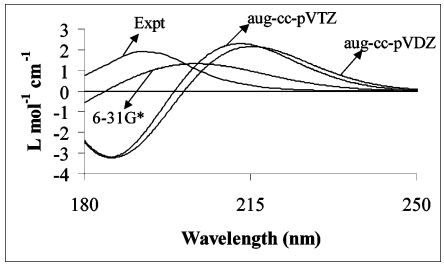


**Figure 7.** Experimental and predicted ECD spectra for (+)-(*R*)-3-chloro-1-butyne. The experimental spectrum is plotted from data taken from ref 39. Predicted spectra were obtained with the B3LYP functional and 6-31G*, aug-cc-pVDZ, and aug-cc-pVTZ basis sets. The ECD spectrum obtained with the 6-31++G(2d,2p) basis set (not shown) is identical to that obtained with the aug-cc-pVTZ basis set.

An alternate approach to determine wavelength correction is to compare the experimental and theoretical ECD spectra and deduce[33] the wavelength shift needed for theoretical spectra to match the corresponding experimental ECD spectra. Such wavelength corrections should be incorporated in determining the quantitative deviations between experimental and predicted optical rotation magnitudes.

From the discussion in this article, it becomes apparent that for practical applications of theoretical optical rotation predic-

tions, the availability of both experimental ECD and ORD is important. If experimental ORD is not available, it can be generated from the corresponding experimental ECD spectrum. The advantage of KK transform (eq 28) for this purpose is that the digitized experimental ECD data can be used as such and the same algorithm can be used for converting theoretical ECD into ORD in both nonresonant and resonant regions.

## Conclusions

Three different numerical integration methods for the application of KK transform have been compared and analyzed for the first time. It was found that the methods suggested by Moscowitz and Ohta and Ishida provide equivalent results, with the latter method being general and suitable for converting both experimental and theoretical ECD data. For quantum mechanical ORD predictions, the KK transform method has been evaluated by comparing the results obtained with KK transform and linear response methods. For three molecules, which exhibit monosignate ORD in the nonresonant long wavelength region, the KK transform of ECD associated with the lowest energy electronic transition yielded essentially the same results as those obtained with the linear response method. For molecules that exhibit bisignate ORD in the nonresonant long wavelength region, the KK transform method may not be successful. For qualitatively reproducing the ORD in the resonant region, the KK transform method offers the advantage of lower computational requirements. The results presented in this paper provide a convenient approach to convert both experimentally observed and theoretically calculated ECD spectra into corresponding ORD, using a single KK transform algorithm. It is hoped that these results will encourage further ORD studies both in experimental and theoretical directions.

**Acknowledgment.** I thank Jiangtao He and Ana G. Petrovic for some of the calculations and the National Science Foundation (CHE0092922) for funding.

**Supporting Information Available:** Tables of rotational strengths for electronic transitions in (*R*)-3-chloro-1-butyne, (*R*)-3-methylcyclohexanone, (*R*)-3-methylcylopenatnone, and (*S*)-3,3,3′,3′-tetramethyl-1,1′-spirobi[3H,2,1]-benzoxaselenole. This material is available free of charge via the Internet at http://pubs.acs.org.

## References and Notes

(1) Lowry, T. M. *Optical Rotatory Power*; Dover Publications Inc.: New York, 1964.

(2) Djerassi, C. *Optical rotatory dispersion*, McGraw-Hill: New York, 1960.

(3) (a) Berova, N.; Nakanishi, K.; Woody, R. W. *Circular dichroism: Principles and Applications*; John Wiley & Sons: New York, 2000. (b) Harada, N.; Nakanishi, K. *Circular Dichroic Spectroscopy: Excition Coupling in Organic Stereochemistry*; University Science Books: Mill Valley, CA, 1983.

(4) (a) Woody, R. W. In *Circular dichroism and the conformational analysis of biomolecules*; Fasman, G. D., Ed.; Plenum: New York, 1996. (b) Lightner, D. A.; Gurst, J. E. *Organic Conformational Analysis and Stereochemistry from Circular Dichroism Spectroscopy*; John Wiley & Sons: New York, 2000.

(5) Moscowitz, A. *Adv. Chem. Phys.* **1962**, *4*, 67−112.

(6) Emeis, C. A.; Oosterhoff, L. J.; De Vries, G. *Proc. R. Soc. London* **1967**, *A297*, 54−65.

(7) (a) Cassim, J. Y.; Yang, J. T. *Biopolymers* **1970**, *9*, 1475−1502. (b) Cassim, J. Y.; Yang, J. T. *Biochemistry* **1969**, *8*, 1947−1951. (c) Carver, J. P.; Shechter, E.; Blout, E. R. *J. Am. Chem. Soc.* **1966**, *88*, 2550−2561. (d) Detar, D. F. *Anal. Chem.* **1969**, *41*, 1406−1408. (e) Krueger, W. C.; Pschigoda, L. M. *Anal. Chem.* **1971**, *43*, 675−677.

(8) Polavarapu, P. L. *Mol. Phys.* **1997**, *91*, 551−554.

(9) (a) Polavarapu, P. L. *Chirality* **2002**, *14*, 768−781. Polavarapu, P. L. *Chirality* **2003**, *15*, 284−285. (b) Crawford, T. D. *Theor. Chem. Acc.*, in press.

(10) (a) Polavarapu, P. L.; Zhao, C. *Chem. Phys. Lett.* **1998**, *296*, 105−110. (b) Kondru, R. K.; Wipf, P.; Beratan, D. N. *J. Am. Chem. Soc.* **1998**, *120*, 2204−2205. (c) Giorgio, E.; Minichino, C.; Viglione, R. G.; Zanasi, R.; Rosini, C. *J. Org. Chem.* **2003**, *68*, 5186−5192.

(11) (a) Yabana, K.; Bertsch, G. F. *Phys. Rev. A* **1999**, *60*, 1271−1279. (b) Stephens, P. J.; Devlin, F. J.; Cheeseman, J. R.; Frisch, M. J. *J. Phys. Chem. A* **2001**, *105*, 5356−5371. (c) Grimme, S. *Chem. Phys. Lett.* **2001**, *339*, 380−388. (d) Ruud, K.; Helgaker, T. *Chem. Phys. Lett.* **2002**, *352*, 533−539. (e) Autschbach, J.; Patchkovskii, S.; Ziegler, T.; van Gisbergen, S. J. A.; Baerends, E. J. *J. Chem. Phys.* **2002**, *117*, 581−592.

(12) (a) Ruud, K.; Stephens, P. J.; Devlin, F. J.; Taylor, P. R.; Cheeseman, J. R.; Frisch, M. J. *Chem. Phys. Lett.* **2003**, *373*, 606−614. (b) Tam, M. C.; Russ, N. J.; Crawford, T. D. *J. Chem. Phys.* **2004**, *121*, 3550−3557. (c) Pedersen, T. B.; Koch, H.; Boman, L.; Sanchez de Meras, A. M. J. *Chem. Phys. Lett.* **2004**, *393*, 319−326.

(13) (a) *Gaussian 03*; Gaussian Inc.: Pittsburgh, PA, 2003; www.Gaussian.com; (b) *Dalton, a molecular electronic structure program*; 2001; www.kjemi.uio.no/software/dalton. (c) *Turbomole*, 2002, www.turbomole.com. (d) *PSI 3.2*, 2003; www.psicode.org. (e) *Amsterdam Density functional program*; www.scm.com.

(14) Polavarapu, P. L.; Zhao, C. *J. Am. Chem. Soc.* **1999**, *121*, 246−247. (b) Giorgio, E.; Viglione, R. G.; Zanasi, R.; Rosini. C. *J. Am. Chem. Soc.* **2004**, *126*, 12968−12976.

(15) Norman, P.; Ruud, K.; Helgaker, T. *J. Chem. Phys.* **2004**, *120*, 5027−5035.

(16) (a) Specht, K. M.; Nam, J.; Ho, D. M.; Berova, N.; Kondru, R. K.; Beratan, D. N.; Wipf, P.; Pascal, R. A., Jr.; Kahne. D. *J. Am. Chem. Soc.* **2001**, *123*, 8961−8966. (b) Polavarapu, P. L. *Angew. Chem., Int. Ed.* **2002**, *41*, 4544−4546. (c) Crassous, J.; Jiang, Z.; Schurig, V.; Polavarapu, P. L. *Tetrahedron: Asymmetry.* **2004**, *15*, 1995−2001. (d) Crawford, T. D.; Owens, L. S.; Tam, M. C.; Schreiner, P. R.; Koch, H. *J. Am. Chem. Soc.* **2005**, *127*, 1368−1369. (e) Rinderspacher, B. C.; Schreiner, P. R. *J. Phys. Chem. A* **2004**, *108*, 2867−2870.

(17) Bak, K. L.; Hansen, A. E.; Ruud, K.; Helgaker, T.; Olsen, J.; Jorgensen, P. *Theor. Chim. Acta* **1995**, *90*, 441.

(18) (a) Grimme, S. *Chem. Phys. Lett.* **1996**, *259*, 128−137. (b) Pecul, M.; Ruud, K.; Helgaker, T. *Chem. Phys. Lett.* **2004**, *388*, 110−119. (c) Autschbach, J.; Ziegler, T.; van Gisbergen, S. J. A.; Baerends, E. J. *J. Chem. Phys.* **2002**, *116*, 6930−6940.

(19) (a) Pedersen, T. B.; Koch, H.; Ruud, K. *J. Chem. Phys.* **1999**, *110*, 2883−2892. (b) Diedrich, C.; Grimme, S. J. *Phys. Chem. A* **2003**, *107*, 2524−2539.

(20) (a) Furche, F.; Ahlrichs, R.; Wachsmann, C.; Weber, E.; Sobanski, A.; Vogtle, F.; Grimme, S. *J. Am. Chem. Soc.* **2000**, *122*, 1717−1724. (b) Stephens, P. J. McCann, D. M.; Devlin, F. J.; Cheeseman, J. R.; Frisch, M. J. *J. Am. Chem. Soc.* **2004**, *126*, 7514−7521. (c) Petrovic, A. G.; He, J.; Polavarapu, P. L.; Xiao, L. S.; Armstrong, D. W. *Org. Biomol. Chem.* **2005**, *3*, 1977−1981.

(21) Meijere, A. D.; Khlebnikov, A. F.; Kozhushkov, S. I.; Kostikov, R. R.; Schreiner, P. R.; Wittkopp, A.; Rinderspacher, C.; Menzel, H.; Yufit, D. S.; Howard, J. A. K. *Chem.—Eur. J.* **2002**, *8*, 828−842.

(22) Barron, L. D. *Molecular Light Scattering and Optical Activity*, 2nd ed.; Cambridge Univ Press: Cambridge, U.K., 2004.

(23) Polavarapu, P. L. In *Fourier Transform Infrared Spectroscopy*; Ferraro, J. R., Basile, L. J., Eds.; Academic Press: New York, 1985; Vol. 4, p 64.

(24) Moscowitz, A. In *Optical rotatory dispersion*; Djerassi, C., Ed.; McGraw-Hill: New York, 1960; pp 150−177.

(25) Faulkner, T. R. Ph.D thesis, University of Minnesota, 1976.

(26) Eliel, E. L.; Wilen, S. H.; Doyle, M. P. *Basic Organic Stereochemistry*; Wiley: New York, 2001.

(27) Buckingham, A. D.; Longuet-Higgins, G. C. *Mol. Phys.* **1968**, *14*, 63−72.

(28) (a) Olsen, J., Jorgensen, P. In *Modern electronic structure theory, Part II*; Yarkony, D. R., Ed.; World Scientific: Singapore, 1995.

(29) Ohta, K.; Ishida, H. *Appl. Spectrosc.* **1988**, *42*, 952−957.

(30) Wiberg, K. B.; Wang, Y. G.; Murphy, M. J.; Vaccaro, P. H. *J. Phys. Chem. A* **2004**, *108*, 5559−5563.

(31) Petrovic, A. G.; Polavarapu, P. L.; Drabowicz, J.; Zhang, Y.; McConnell, O. J.; Duddeck, H. *Chem.—Eur. J.*, in press

(32) (a) Ruud, K.; Zanasi, R. *Angew. Chem.*, in press; (b) Kongsted, J.; Pedersen, T. B.; Strange, M.; Osted, A.; Hansen, A. E.; Mikkelsen, A. V.; Pawlowski, F.; Jorgensen, P.; Hattig, C. *Chem. Phys. Lett.* **2005**, *401*, 385−392. (c) Tam, M. C.; Russ, N. J.; Crawford, D. T. *J. Chem. Phys.* **2004**, *121*, 3550−3557. (d) Giorgio, E.; Rosini, C.; Viglione, R. G.; Zanasi, R. *Chem. Phys. Lett.* **2003**, *376*, 452−456. (e) Miller, T.; Wiberg, K. B.; Vaccaro, P. H. *J. Phys. Chem.* A. **2000**, *104*, 5959−5968.

(33) Polavarapu, P. L.; He, J.; Crassous, J.; Ruud, K. *ChemPhysChem*, in press.

(34) Stephens, P. J.; McCann, D. M.; Cheeseman, J. R.; Frisch, M. J. *Chirality*, **2005**, *17*, S52−S64.

(35) Cheeseman, J. R.; Frisch, M. J.; Devlin, F. J.; Stephens, P. J. *J. Phys. Chem. A.* **2000**, *104*, 1039−1046.

(36) Mennucci, B.; Tomasi, J.; Cammi, R.; Cheeseman, J. R.; Frisch, M. J.; Devlin, F. J.; Gabriel, S.; Stepehens, P. J. *J. Phys. Chem. A* **2002**, *106*, 6102−6113.

(37) Polavarapu, P. L.; Petrovic, A.; Wang, F. *Chirality* **2003**, *15*, S143−S149; **2003**, 15, 801.

(38) Ruud, K.; Taylor, P. R.; Astrand, P. O. *Chem. Phys. Lett.* **2001**,*337*, 217−223.; (b) Wiberg, K. B.; Vaccaro, P. H.; Cheeseman, J. R. *J. Am. Chem. Soc.* **2003**, *125*, 1888−1896.; (c) Wiberg, K. B. Wang, Y. G.; Vaccaro, P. H.; Cheeseman, J. R.; Trucks, G.; Frisch, M. J. *J. Phys. Chem. A* **2004**, *108*, 32−38.

(39) (a) Bauernschmitt, R.; Ahlrichs, R. *Chem. Phys. Lett.* **1996**, *256*, 454−464. (b) Furche, F.; Ahlrichs, R. *J. Am. Chem. Soc.* **2002**, *124*, 3804−3805.

(40) He, J.; Petrovic, A.; Polavarapu, P. L. *J. Phys. Chem. A* **2004**, *108*, 1671−1680.